

## Supplementary Information

### Synthesis of Chiral Metal Oxide Complexes with Tunable Electron Transition-Based Optical Activity

<sup>5</sup> Liguo Ma<sup>1</sup>, Yingying Duan<sup>1</sup>, Yuanyuan Cao<sup>1</sup>, Shunsuke Asahina<sup>2</sup>, Zheng Liu<sup>3</sup> and Shunai Che<sup>1,\*</sup>

#### Experimental section

##### Materials

<sup>10</sup> Zirconium oxychloride, ferric chloride, manganese acetate (SCRC, China) and TDA (TCI, Japan) were purchased. All N-acylamino acids (N-AAA) were synthesized according to the previous report. All chemicals were used as received without further purification.

##### Methods

<sup>15</sup> The helical metal oxides complex nanofibres can be synthesised over a wide range of molar compositions of C<sub>18</sub>-D-Glu:TDA:Metal precursor:MeOH:H<sub>2</sub>O = 1:7.5:x:5312:55962, where x can be adjusted in the range of 2~10. A temperature of 50~65 °C is favourable for the formation of helical fibres. In a typical synthesis, C<sub>18</sub>-D-Glu (0.03 g, 0.08 mmol) was dissolved in a mixture of methanol (13.6 g) and deionised water (80 ml) while stirring at room temperature. After the mixture was stirred for 10 min, TDA (0.29 g, 75% in isopropanol) and  
<sup>20</sup> zirconium oxychloride (0.4606g, 33% in methanol) were added to the mixture with stirring at 60 °C, respectively. The mixture was allowed to react at 60 °C with stirring for 2 h. The products were collected by centrifugal separation and dried by freeze drying at -60 °C, which resulted in a pale yellow powder. All organics in this product were removed by calcination at 550 °C, and inorganic oxides complex crystalline were obtained. The method for the synthesis of other helical metal oxides complex nanofibres using C<sub>18</sub>-L-Glu or C<sub>18</sub>-D-Glu  
<sup>25</sup> are the same as the above and other inorganic precursors are ferric chloride and manganese acetate, respectively.

##### Characterization

The morphology of the chiral metal oxide complex nanofibres were observed with SEM (JEOL JSM-7401F) with an accelerating voltage of 1.0 kV. HRTEM images were taken with a JEOL JEM-2100 microscope  
<sup>30</sup> operating at 200 kV. Powder X-ray diffraction patterns were recorded on a Rigaku X-ray diffractometer D/MAX-2200/PC equipped with Cu K $\alpha$  radiation (40 kV, 20 mA). Ultraviolet and DRUV spectra were taken by using a Shimadzu UV-2450 spectropolarimeter fitted with DRUV apparatus. CD and DRCD spectra were taken by using a JASCO J-815 spectropolarimeter fitted with DRCD apparatus.

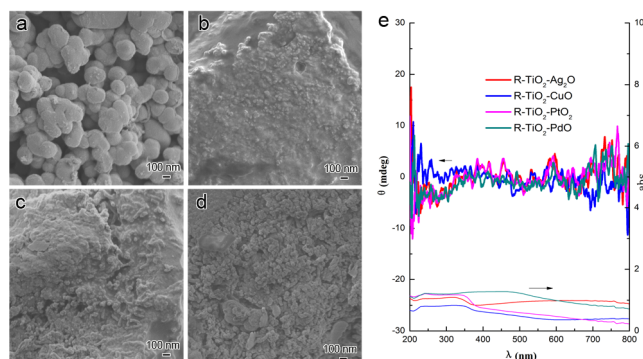


**Figure S1.** SEM images, DRUV-Vis and DRCD spectra of R-TiO<sub>2</sub>-Ag<sub>2</sub>O, R-TiO<sub>2</sub>-CuO, R-TiO<sub>2</sub>-PtO<sub>2</sub>, and R-TiO<sub>2</sub>-PdO. The molar composition for the synthesis was C<sub>18</sub>-D-Glu:TDA:Metal: MeOH:H<sub>2</sub>O=1:7.5:5:5312:55962, the metal sources are AgNO<sub>3</sub>, Cu(NO<sub>3</sub>)<sub>2</sub>•3H<sub>2</sub>O, K<sub>2</sub>PtCl<sub>6</sub>, and K<sub>2</sub>PdCl<sub>6</sub>, respectively.

5

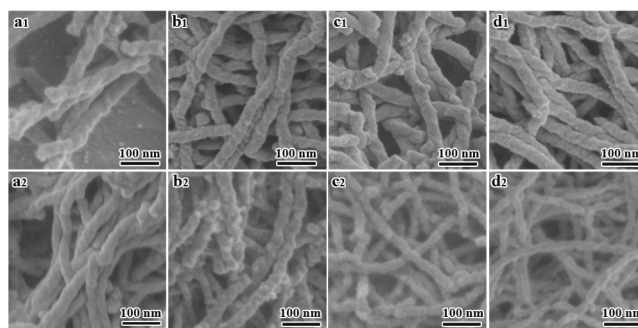


**Figure S2.** SEM images of the as-made (a<sub>1</sub>-d<sub>1</sub>) and calcined chiral metal oxides (a<sub>2</sub>-d<sub>2</sub>); L-ZrO<sub>2</sub> (a<sub>1</sub> and a<sub>2</sub>), L-TiO<sub>2</sub>-ZrO<sub>2</sub> (b<sub>1</sub> and b<sub>2</sub>), L-TiO<sub>2</sub>-Fe<sub>2</sub>O<sub>3</sub> (c<sub>1</sub> and c<sub>2</sub>), and L-TiO<sub>2</sub>-Mn<sub>2</sub>O<sub>3</sub> (d<sub>1</sub> and d<sub>2</sub>). The synthesis compositions were: (a<sub>1</sub>) C<sub>18</sub>-L-Glu:ZrOCl<sub>2</sub>•8H<sub>2</sub>O:MeOH:H<sub>2</sub>O=1:7.5:5312:55962. (b<sub>1</sub>-d<sub>1</sub>) C<sub>18</sub>-L-Glu:TDA:Metal:MeOH:H<sub>2</sub>O=1:7.5:5:5312:55962, the metal sources are ZrOCl<sub>2</sub>•8H<sub>2</sub>O, FeCl<sub>3</sub>•6H<sub>2</sub>O and C<sub>4</sub>H<sub>6</sub>MnO<sub>4</sub>•4H<sub>2</sub>O, respectively.

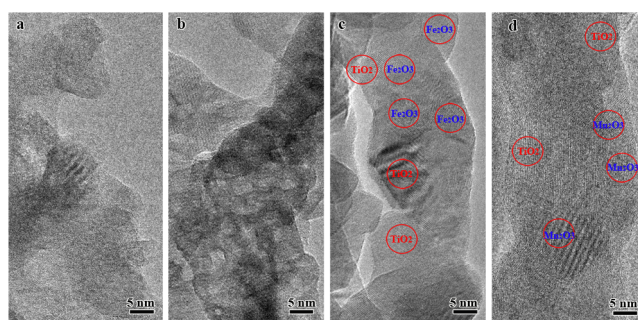


**Figure S3.** TEM images of calcined chiral metal oxides and complexes shown in Fig.1. R-ZrO<sub>2</sub> (a), R-TiO<sub>2</sub>-ZrO<sub>2</sub> (b), R-TiO<sub>2</sub>-Fe<sub>2</sub>O<sub>3</sub> (c), and R-TiO<sub>2</sub>-Mn<sub>2</sub>O<sub>3</sub> (d). The lattice fringes of  $d=1.4$  Å match that of the (215) crystallographic planes of anatase-TiO<sub>2</sub>; the lattice fringes of  $d=1.6$ , 1.8, and 2.2 Å match that of the (116), (024), and (113) crystallographic planes of hematite  $\alpha$ -Fe<sub>2</sub>O<sub>3</sub>. The lattice fringes of  $d=1.7$  Å match that of the (044) crystallographic planes of  $\alpha$ -Mn<sub>2</sub>O<sub>3</sub>. These crystallographic planes have been clearly identified in the figures.

15

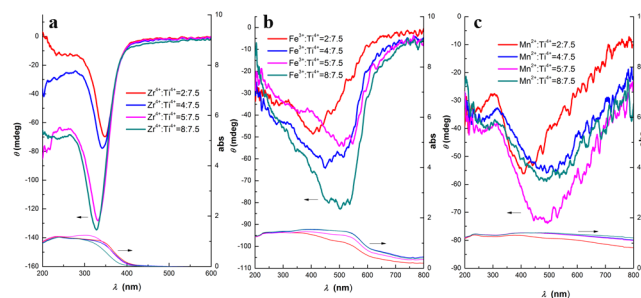


**Figure S4.** DRUV-Vis and DRCD spectra of calcined chiral metal oxides complexes synthesized with different ratio of metal ion to  $\text{Ti}^{4+}$ .

5 In Fig. S4a, with increasing molar ratio of  $\text{Zr}^{4+}/\text{Ti}^{4+}$ , the DRCD spectra of the metal oxides complex were gradually blue-shifted due to the  $\text{ZrO}_2$  with absorption band in the range of 200-260 nm shorter than  $\text{TiO}_2$ . In Fig. S4b and Fig. S4b, with increasing of molar ratio of  $\text{Fe}^{3+}/\text{Ti}^{4+}$  and  $\text{Mn}^{2+}/\text{Ti}^{4+}$ , the DRCD spectra of the metal oxides complex were gradually red-shifted because of  $\text{Fe}_2\text{O}_3$  and  $\text{Mn}_2\text{O}_3$  with absorption band in the range of 400-600 nm longer than  $\text{TiO}_2$ .